

collateral growth in the treatment of CTOs with no suitable revascularization option.

Funding Acknowledgements: National Natural Science Foundation of China (grant 81300095)

P6405

Implications of the local haemodynamic forces on plaque morphology: A serial intravascular ultrasound and optical coherence tomography analysis

A. Ramasamy¹, C.V. Bourantas¹, A. Sakellarios², A. Karagiannis³, T. Zanchin⁴, K. Yamaji⁴, M. Taniwaki⁴, D. Heg³, D.I. Fotiadis², A. Baumbach¹, L.K. Michalis⁵, P.W. Serruys⁶, H.M. Garcia-Garcia⁷, S. Windecker⁴, L. Raber⁴. ¹Barts Health NHS Trust, Department of Cardiology, London, United Kingdom; ²University of Ioannina, Department of Materials Science and Engineering, Ioannina, Greece; ³Bern University Hospital, CTU Bern, Institute of Social and Preventive Medicine (ISPM), Bern, Switzerland; ⁴Bern University Hospital, Department of Cardiology, Bern, Switzerland; ⁵University of Ioannina, 2nd Department of Cardiology, Medical School, Ioannina, Greece; ⁶Imperial College London, International Centre for Circulatory Health, NHLI, London, United Kingdom; ⁷MedStar Research Institute, Section of Interventional Cardiology, Washington, United States of America

Background and introduction: Cumulative evidence has shown that local haemodynamic forces, in particular the endothelial shear stress (ESS) regulate atherosclerotic evolution and enable to predict lesions that may cause future cardiovascular events. However, there is limited clinical evidence surrounding the effect of ESS on plaque morphology.

Purpose: To evaluate the implications of ESS on plaque morphology and their role on the dynamic changes in plaque phenotype.

Methods: Patients admitted with ST-elevation myocardial infarction who had successful revascularisation and serial 3-vessel intravascular ultrasound virtual histology (IVUS-VH) and optical coherence tomography (OCT) imaging at baseline and at 13 months follow-up were included in the present analysis. Plaque morphology was derived from the IVUS-VH and OCT data at these two time points. The IVUS data were used to reconstruct coronary artery anatomy of the non-culprit vessels and the ESS distribution was estimated in 3mm segments. Plaque progression was defined as the presence of two or three out of the following criteria: a reduction in lumen area, an increase in plaque burden and change of plaque morphology to a more vulnerable phenotype.

Results: Sixty nine vessels (497 3mm segments) were included in the present analysis. A total of 63 out of the 117 segments with a normal plaque morphology (i.e. adaptive and pathological intimal thickening), 90 out of the 208 segments with a fibrotic and fibrocalcific phenotype and 65 out of 172 segments with advanced plaque morphology (i.e. calcified and non-calcified fibroatheromas and thin cap fibroatheromas) exhibited disease progression at follow-up. Segments with a normal morphology that exhibited disease progression had a larger lumen area (9.3mm² vs. 7.5mm², P=0.021), necrotic core burden (1% vs. 0%, P=0.045) and were exposed to lower ESS (0.83Pa vs. 1.29Pa, P=0.008) comparing to those that did not progress at follow-up. Segments with a fibrotic/fibrocalcific phenotype that exhibited disease progression had a larger lumen area (8.7mm² vs. 7.1mm², P=0.001) and fibrotic tissue burden (34% vs. 30%, P=0.017), a smaller plaque burden (43% vs. 49%, P=0.002), increased incidence of neovessels (14% vs. 6%, P=0.039) and were exposed to lower ESS (1.08Pa vs. 1.52Pa, P=0.003) comparing to the segments that did not progress at follow-up. The only difference between the 3mm segments with advanced plaques that demonstrated disease progression at follow-up compared with segments without progression was in the ESS distribution (1.48Pa vs. 1.85Pa, P=0.030).

Conclusion(s): The frequency and predictors of atherosclerotic disease progression vary across different plaque morphologies. Low ESS appears to be associated with plaque progression, independent of plaque morphology even in plaques with a plaque burden >40%.

P6406

Clinical course and predictors of ischemic mitral regurgitation in patients with inferoposterior and anterior myocardial infarction

A.L. Chilingaryan, K.G. Adamyan, L.G. Tunyan, L.R. Tumasyan, N.G. Mkrtychyan. Institute of Cardiology, Yerevan, Armenia

Ischemic mitral regurgitation (IMR) is a common complication of myocardial infarction (MI) and even being mild significantly affects survival. We studied clinical course and predictors of IMR in patients (pts) with first inferoposterior (IPMI) and anterior (AMI) MI considering its progressive nature.

Methods: We studied 156 pts (52 women) with first acute IPMI (77) or AMI (79) 57±5 years revascularized within 12 hours of symptoms onset without history of ischemic heart disease, valvular disease, atrial fibrillation and diabetes mellitus. Age and sex matched 50 healthy subjects served as control. Conventional and speckle tracking (ST) EchoCG were performed in 7 and 180 day follow up. Mitral valve tenting area (TA), coaptation height (CH), apical displacement (AD) of both papillary muscles (PMPM, ALPM), lateral (LD) and posterior (PD) displacements of both PMs, mitral annulus (MA) contraction (MAC) from MA areas (MAA) were measured as previously described. MAA was calculated by ellipse formula. LV sphericity index (SI) was calculated as $[ESV/(4/3)\pi r^3] \times 100\%$, where r = LV long

axis diameter/2. Global (G) and infarcted segmental (IS) LV longitudinal strain (LS), PMPM LS, ALPM LS were measured by ST EchoCG. Systolic dyssynchrony of PMs (SDPM) was measured as a difference of time to peak LS of PMs. At least mild IMR was defined by regurgitant orifice area (ROA) <0.2 cm². IMR degree change was considered as changes of ROA ≥0.1 cm².

Results: IMR was more frequent in IPMI (42 vs 28%). Pts with IPMI and IMR had worse values of IS LS, preserved PMPM LS, more PMPM PD and systolic MAA than IPMI pts without IMR in 7 day (ISLS -12.7±4 vs -9.2±6%, p<0.02; PMPM LS -13.8±1.3 vs -11.3±1.4%, p<0.02; PMPM PD 3.2±0.9 vs 4.5±1.9 mm, p<0.03; MAA_{syst} 467,3±117,8 vs 564,6±114,2 mm², p<0.02). AMI pts with IMR had worse GLS, more MAA_{syst} and SI than pts without IMR in 7 day (GLS -15.2±1.5 vs -14.6±1.8, p<0.03; MAA_{syst} 418.4±113.6 vs 486.7±117.6 mm², p<0.04). 37.5% IPMI pts had IMR decrease in 180 day. No IPMI patient without IMR on 7 day develop IMR during follow up. 19.3% AMI pts developed IMR in 180 day, and 45.5% pts had IMR decrease. IPMI pts with IMR in 180 day had similar (with IPMI pts without IMR) differences in parameters, observed on 7 day. AMI pts with IMR had greater SI, SDPM, and more AD of PMs. MAA_{syst} than no IMR AMI pts (SI 17±5 vs 25±14%, p<0.002; SDPM 23±10 vs 39±14 ms, p<0.005; AD PMPM 3,32±0,87 vs 4,17±0,90 cm, p<0.02; AD ALPM 3,31±0,92 vs 3,97±0,97 cm, p<0.02; MAA_{syst} 621,3±142,7 vs 474.8±122.5 mm², p<0.003). Logistic regression analysis defined TA in both MI types, SI, SDPM in AMI and PD PMPM in IPMI as an independent predictors of IMR (TA OR=2.3 95% CI=1.11–5.10, p<0.02; SI OR=2.9; 95% CI=1.32–6.55, p<0.01; SDPM OR=2.8; 95% CI=1.37–6.58, p<0.01; PD PMPM OR=3.2; 95% CI=1.36–7.83; p<0.01).

Thus clinical course and mechanisms of IMR are different in pts with IPMI and AMI. More local LV changes in IPMI and more global LV remodeling in AMI are responsible for IMR.

P6407

A new method for the correct evaluation of wall shear stress in bifurcations: fusion of three-dimensional angiography and two-vessel OCT

A. Karanasos¹, K. Toutouzias¹, I. Andrikos², A. Sakellarios², P. Siogkas², G. Rigas², A. Synetos¹, G. Latsios¹, E. Tsiamis¹, L. Michalis³, D. Fotiadis², D. Tousoulis¹. ¹Hippokraton Hospital, University of Athens, Athens, Greece; ²University of Ioannina, Unit of Medical Technology and Intelligent Information Systems, Ioannina, Greece; ³University of Ioannina Medical School, Department of Cardiology, Ioannina, Greece

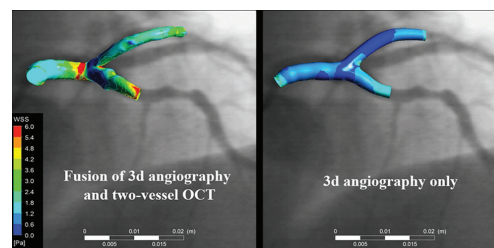
Background: Coronary hemodynamics have emerged as a potential factor mediating atherosclerotic plaque progression and healing response after stent implantation. Although computation of hemodynamic parameters is of utmost importance in coronary bifurcations, current methodologies for such evaluation are hampered as they do not incorporate high-resolution imaging information from both side-branches.

Purpose: We developed a methodology for the in vivo assessment of wall shear stress (WSS) in the left main bifurcation by fusing information from 3d angiography with intravascular optical coherence tomography (OCT) data.

Methods: Patient-specific data from 3 human patients undergoing coronary angiography and OCT for diagnostic purposes were used. Two angiographic views of the left main bifurcation with an angle >30° were recorded and used for the development of the 3d pullback path of the bifurcation. Two separate frequency domain OCT pullbacks were performed, one from the LAD and one from the LCx artery. Landmarks visible both in angiography and OCT were annotated on each angiographic projection by an expert OCT reader, in order to define the region of interest for both pullbacks. The lumen borders of the FD-OCT sequence were then backprojected perpendicularly to the 3d angiographic catheter path after adjusting the orientation of OCT frames. A separate model was reconstructed for comparison purposes using information from 3d angiography only. Computational fluid dynamics were then applied to the both models using similar boundary conditions and WSS was calculated.

Results: All three left main bifurcations were successfully reconstructed with both algorithms. Comparison of the two algorithms resulted in significantly different

Differences in WSS between the proposed				
	Overall	Main Vessel	Main branch	Side branch
Percent differences in mean WSS between the two methods	59.14±57.17	77.26±66.03	77.42±30.05	50.74±13.86
Percent differences in SD of WSS between the two methods	66.55±71.12	85.37±80.90	101.94±24.40	36.78±35.47



Picture 1